Study on fracture behavior of NiTi Alloy by the digital image correlation method

Study on fracture behavior of NiTi Alloy by the digital image correlation method

L Y Ma, Y J Li* and G Han

School of Civil Engineering and Architecture, University of Jinan, Jinan 250022, China

*E-mail: cea_liyj@ujn.edu.cn

Abstract. Due to its unique super-elasticity and shape memory effect, NiTi alloy has been widely used in aerospace, civil engineering, and other fields. As it is well known, the defect of the material itself will affect its mechanical properties and service life, especially the fracture properties. To study the influence of the defect on the fracture properties of NiTi alloy, in this paper, the relationships between the stress intensity factor (SIF), stress values, and the number of fitting terms of two different NiTi alloys are investigated within the framework of fracture mechanics approach. The results obtained strongly indicate that SIF values of two specimens with different defects gradually increase with the stress; when the number of fitting terms reaches 8, the error is stable within 2%. Moreover, the SIF in both specimens tends to be stable with the increase in the number of fitting terms.

1. Introduction

Due to the needs of structural design, material processing, and other factors, the structure always contains a specific defect. The presence of defects will affect the mechanical properties of the material, and the change of the mechanical properties of the material varies with the geometrical shape of the defect. Therefore, it is necessary to study the fracture mechanics of defective components. In fracture mechanics, the stress intensity factor is an important parameter to characterize the fracture properties of materials. Dally [1] used the resistance strain gauge method to test the stress intensity factor (SIF) theory of aluminum plates. Xi [2] used the photoelastic method to study the stress intensity factor of the I-type crack tip of polyester photoelastic materials. At present, the digital image correlation (DIC) method is most widely in the SIF measurement.

NiTi alloy [3] has a unique and excellent hyperelastic and shape memory effect, and its stress-strain curve [4] has visible hysteresis characteristics (caused by the internal phase transition process of the material), does not cause damage to the material, and the NiTi alloy also has excellent corrosion resistance [5] and fatigue resistance [6]. Due to its unique effect, NiTi alloy has been widely used in various fields, such as aerospace [7], civil engineering [8], and other fields. The defects in the material and scratches formed during its processing are the factors that cause the SIF variation. Therefore, it is of theoretical and engineering significance to study the SIF of NiTi alloy defect specimen for structural design and safety reliability evaluation. Given this, the tensile tests of NiTi alloys with different defects have been carried out, and the variation trend of SIF with the change of stress and the number of fitting terms has been obtained. To get more accurate measurement data, this paper optimizes the DIC carrier, speckle, and obtains the production parameters of higher quality speckle.

2. Extraction of SIF based on DIC

2.1. Principle of DIC

It is the basic principle of DIC to compare the gray feature of speckle image before and after deformation. The tested surface needs to have enough recognizable mark points, generally by spraying black and white paint spots on the specimen surface as a speckle mark point, and assume that the deformation of these speckles is the deformation of the specimen itself.

According to the study [9], the displacement expressions of the area to be tested are as follows：

$$u_j = \frac{1}{2u}\sum_{n=1}^{\infty} a_n r_j^{\frac{n}{2}}\left[\left(k+\frac{n}{2}+(-1)^n\right)\cos\frac{n}{2}\theta_j - \frac{n}{2}\cos(\frac{n}{2}-2)\theta_j\right] + u^* - \alpha r_j sin\theta_j \quad (1)$$

$$v_j = \frac{1}{2u}\sum_{n=1}^{\infty} a_n r_j^{\frac{n}{2}}\left[\left(k-\frac{n}{2}-(-1)^n\right)\sin\frac{n}{2}\theta_j + \frac{n}{2}\sin(\frac{n}{2}-2)\theta_j\right] + v^* + \alpha r_j cos\theta_j \quad (2)$$

where r and θ are the polar coordinates of any point of the area to be tested, K is the elastic constant; the superscript j represents the j_{th} data point of the n data points, the coordinate is (x_j, y_j); $u^*$and v^* are the rigid body displacement along x-direction and y respectively, α is the in-plane angle.

Expression of SIF obtained from the fracture mechanics is as follows:

$$K_I = \sqrt{2\pi}a_1 \quad (3)$$

Based on formulas (1) and (2), a_1 and other coefficients can be fitted by the displacement obtained by DIC, while SIF (K_I) is calculated by formula (3).

According to works of literature, DIC has the following advantages over other methods of measuring defects:

1) Compared with the resistance strain gauge method [1], it has the advantage of full-field measurement, and sufficient deformation information can be obtained;

2) Compared with the photoelastic method [10], the experimental equipment is simple, and the environmental factors have little influence. It is considered to develop outdoor applications of this measurement method;

3) Compared with the moiré interferometry [11], the equipment is simple, the required magnification is small, and the requirements for light are low;

4) High-speed cameras can be used for dynamic measurements [12] to compensate for the shortcomings of static measurements.

2.2. Speckle optimization

Speckle is the crucial carrier of DIC deformation information. Making high quality and easy to transfer speckle is one of the critical steps to improve the accuracy of DIC measurement. There are mainly two kinds of speckle: natural randomly distributed grayscale [13] and artificially produced spot [14]. In scientific studies, artificial speckles are mostly used, and carbon powder together with paint is mainly used as speckles. However, the average size of the particles is about 5μm, which is too large and easy to be distorted under the depth of field microscope. Therefore, the graphite powder with an average size of about 1.5μm is selected to optimize the fabrication of speckles. In this study, Huaixi Wang's [15] research was used to streamline the production process of speckle.

The speckle production process [16] is shown in figure 1:

1) Determining the ratio of graphite powder to epoxy curing agent, weigh graphite powder, and prepare epoxy curing agent;

2) Mixing the curing agent with the graphite powder, and centrifuging with a centrifuge to obtain a mixture solution;

3) Pouring the solution onto the acrylic plate in the silicone machine, and apply the glue;

4) Stewing release acrylic plate for 24h, curing;

5) Observing the resulting speckle under an optical microscope.

The quality of speckle is influenced by the concentration of epoxy resin and graphite powder, radial velocity and solution curing time, the speed of glue-throwing and the time of glue-throwing. In this

paper, the above factors are optimized to obtain the high-quality speckle, as shown in figure 2, the production parameters, in turn, are 3ml: 0.1g, 2000r/min, 10min, 3500r/min, 50s.

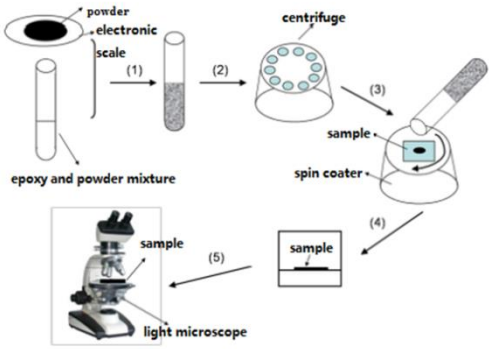

Figure 1. Flowchart of the speckle.

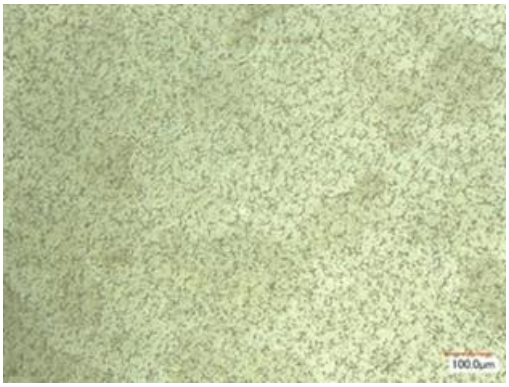

Figure 2. Speckle patterns.

3. Experimental

3.1. Experimental conditions

In this study, two specimens (figure 3) with groove and curved defects were produced, each having a thickness of 1 mm. The specimens with defects were subjected to pre-treatment such as grinding, polishing, etching, etc., and then underwent the tensile tests. The polishing temperature was below 15ºC.

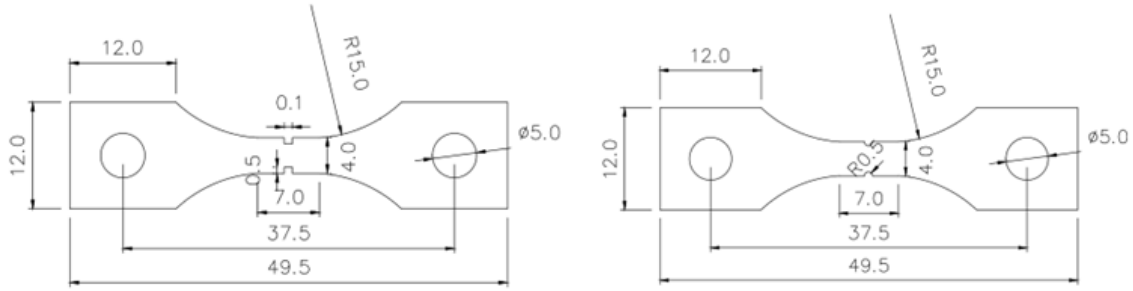

(a) (b)

Figure 3. Specimen geometry (a) with groove notches/defects; (b) with curved notches/defects.

3.2. Experimental method

Each specimen was fixed after the transfer of the speckle, taken a reference image, and then loaded at a rate of 10N/S. During the loading process, images of specimen deformation by forces of 100, 200, 300, 400, 500, and 600 N were recorded. The tensile test was carried out by in-situ loading system as shown in figure 4. The test temperature was 20~28ºC.

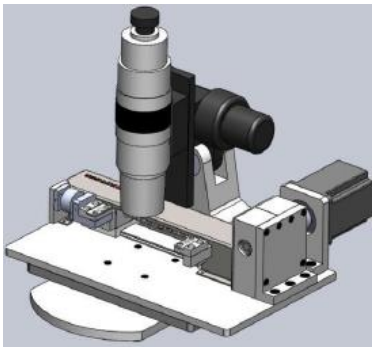

Figure 4. In-situ loading system.

4. Analysis and discussion of experimental results

4.1. Experimental results

The deformed images were processed by DIC to obtain the displacement fields under different stresses. Figure 5 illustrates the displacement fields of two defected specimens at the stress value of 25MPa.

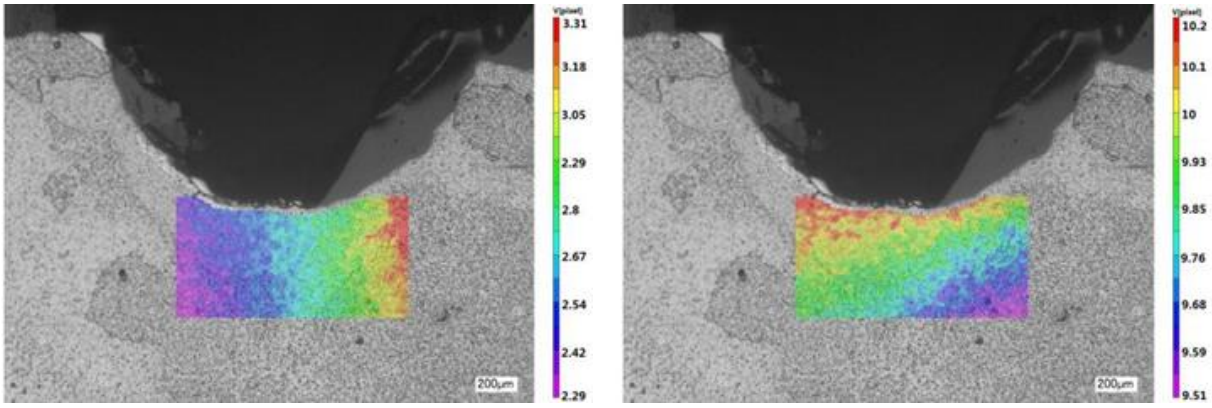

U field V field

(a) Curve-defect displacement field.

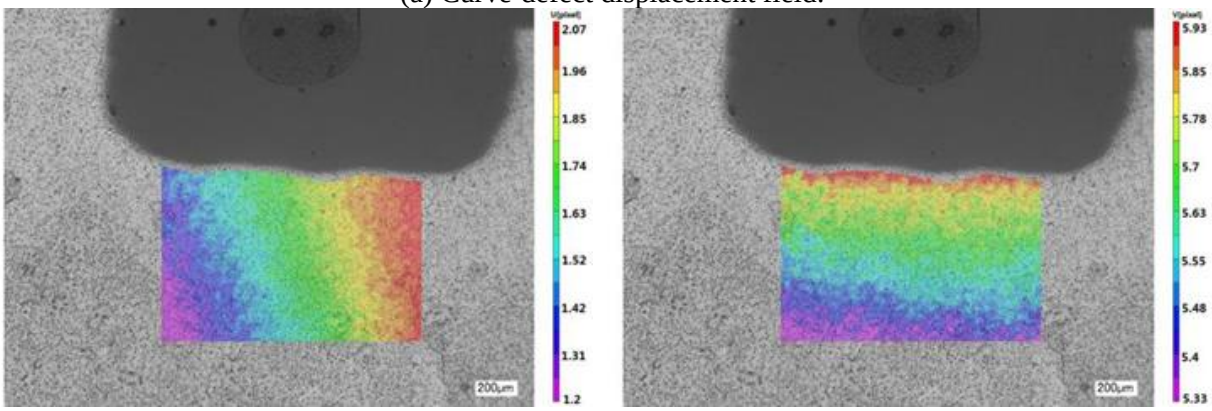

U field V field

(b) Groove-defect displacement field.

Figure 5. The displacement fields of two defected specimens at the stress of 25MPa.

4.2. SIF variation laws

The calculated results are shown in figure 6, where the specimen with curved defects is denoted as specimen 1 and that with grooved defects as specimen 2.

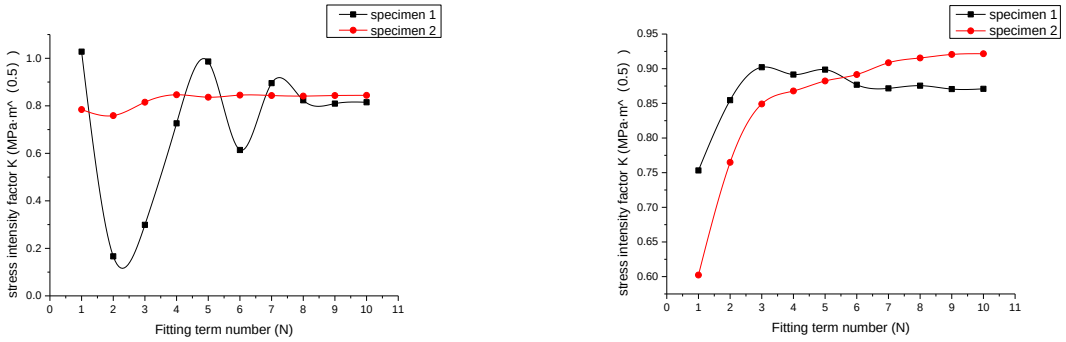

25MPa stress 150MPa stress

(a) SIF values versus the number of fitting terms.

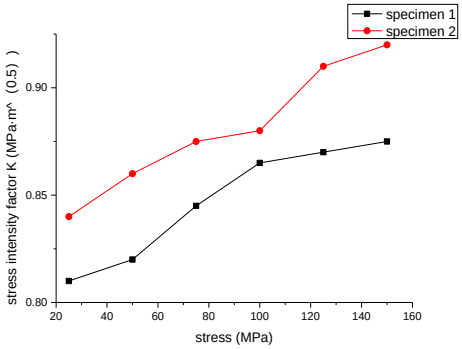

(b) SIF values versus stress.

Figure 6. SIF variation in two specimens.

Table 1. SIF value versus the number of fitting terms at the stress level of 25MPa.

Fitting term number	1	2	3	4	5	8	10	Stable value
Specimen 1	1.028	0.1664	0.299	0.7262	0.9864	0.8232	0.8149	0.81
Specimen 2	0.7843	0.7588	0.8153	0.8466	0.8363	0.8411	0.8441	0.84
Error 1(%)	26.91	79.46	63.09	10.35	21.78	1.63	0.61	/
Error 2(%)	6.63	9.67	2.94	0.79	0.44	0.13	0.49	/

Table 2. SIF value versus the number of fitting terms at the stress level of 150MPa.

Fitting term number	1	2	3	4	5	8	10	Stable value
Specimen 1	0.7532	0.8546	0.9021	0.8916	0.8987	0.8755	0.871	0.875
Specimen 2	0.6023	0.7649	0.8491	0.8679	0.8823	0.9155	0.9216	0.92
Error 1(%)	13.92	2.33	3.10	1.90	2.71	0.06	0.46	/
Error 2(%)	34.53	16.86	7.71	5.66	4.10	0.49	0.17	/

Table 3. SIF values versus stress level

Stress (MPa)	25	50	75	100	125	150
Specimen 1	0.81	0.82	0.845	0.865	0.87	0.875
Specimen 2	0.84	0.86	0.875	0.88	0.91	0.92

4.3. Analysis of SIF variation law

According to the study [17], the NiTi alloy was tested at 28 ºC, and the hyperelastic performance was not apparent before the stress reached 300 MPa. The maximum stress in the experiment was 150 MPa, and the material was still in the elastic range, meeting the underlying assumptions of elastic mechanics.

It is found from figure 6(a) that as the number of fitting terms increases, the fluctuation of SIF value is getting smaller, and tends to be stable after the number of fitting terms reaches 8. As shown in Figure 6(b), the SIF value of the two kinds of defective specimens increases with the increase of the stress, while the SIF value of the groove-shaped specimens is larger.

4.4. Discrete analysis of SIF value

Although the general trend of SIF values is easily identified, the discrete points cannot be ignored.

1) When the stress is 25 MPa, the data input is provided from table 1.

When a single a point is selected from the curved-defect specimen is selected to calculate the SIF value, the error is 26.91%. When two items are selected for the fitting calculation, the error reaches 79.46%. As the number of fitting terms increases, the SIF value gradually approaches a fixed value. When the number of fitting terms reaches 8, the error is controlled within 2%. The variation of the SIF value fitting of the groove-defect specimen is lower during the process of fitting, and is stable within 10%.

2) When the stress is 150 MPa, the data input is provided from table 2.

When the number of fitting terms is less than 5, the SIF value of the curved-defect specimen is larger than that of the groove-defect one, and as the number of fitting items increases, the opposite trend is gradually observed. Finally, the SIF values in both specimens tend to be stable. The error is controlled within 1%.

3) As shown in table 3 and figure 6(b), the SIF value of the two kinds of defective specimens increases with the stress, while the SIF value of the groove-shaped specimens is larger. The process of increasing the value of K has a certain undulation, and when the stress is 100 MPa, the crack growth rate in the groove-defect specimen is slightly reduced, then it continues to increase, while that in the curved-defect one slightly rises first, and then slowly grows.

5. Conclusion

In this paper, the mechanical tests and microstructure analysis of two kinds of defective specimens are carried out. From the results of this study, the following conclusions can be drawn:

- ✓ The calculation of the SIF of NiTi alloy material is controlled by the number of fitting terms. As the number of fitting terms increases, the accuracy of SIF measurements is improved.
- ✓ When assessing the SIF value, the selection of the number of calculation points will affect the result.
- ✓ As the stress increases, the SIF values will rise, and the SIF variation trend in specimens with different defects will become inconsistent. Finally, the SIF values in both specimens tend to be stable and the error is controlled within 1%.

Acknowledgment

The authors are grateful for the financial support of the Project of Shandong Province Higher Educational Science and Technology Program (Grant No. J16LJ12)

References

[1] Dally J W and Sanford R J, 1987. *K I. Exp Mech.*, **27**(4): p. 381-8.
[2] Zhao X, et al., 2017. *Chinese Journal of Engineering*, **39**: 1288-94.
[3] Thierry B, et al., 2000. *J. Biomed. Mater. Res.*, **51**(4): p. 685-93.
[4] Machado G, et al., 2015. *Mater. Des.*, **65**: p. 212-20.
[5] Jamesh M I, et al., 2015. *Corros Sci.*, **97**: p. 126-38.
[6] Pirani C, et al., 2016. *Int Endod J.*, **49**(5): p. 483-93.
[7] Li J F, et al., 2014. *Materials Review*, **28**: 104-8.
[8] Zhuang P, et al., 2015. *Journal of Architecture and Civil Engineering*, **32**: 96-103.
[9] Hao W F, et al., 2015. *Journal of Aeronautical Materials*, **35**: 90-5.
[10] Wang W C and Hwang C H, 1998. *Int J Fracture*, **91**(4): p. 311-21.
[11] Zhang C Y, et al., 2016. *Applied Laser*, **4**: 434-9.
[12] Fan Y F, et al., 2015. *Journal of Experimental Mechanics*, **30**(5): p. 590-8.
[13] Zhao P L, et al., 2017. *China Measurement & Test*, **43**(9): 8-12.
[14] Yu Q, et al., 2017. *Hot Working Technology*, **3**: 1-5.
[15] Wang H, et al., 2012. *Mea Sci Technol.*, **23**(3): p. 035402.
[16] He G L, 2016. *Research on Microscale Digital Image Correlation Methods and Techniques*, Jiangsu University.
[17] Wang X M, et al., 2009. *Superelastic Mechanical Properties and Applications of NiTi Alloys*, Science Press.